nature geoscience

FOCUS | LETTERS

PUBLISHED ONLINE: 24 OCTOBER 2010 | DOI: 10.1038/NGEO991

Seismic hazard of the Enriquillo–Plantain Garden fault in Haiti inferred from palaeoseismology

C. S. Prentice[1]*, P. Mann[2], A. J. Crone[3], R. D. Gold[3], K. W. Hudnut[4], R. W. Briggs[3], R. D. Koehler[5] and P. Jean[6]

The Enriquillo–Plantain Garden fault zone is recognized as one of the primary plate-bounding fault systems in Haiti[1,2]. The strike-slip fault runs adjacent to the city of Port-au-Prince and was initially thought to be the source of the 12 January 2010, M_w 7.0 earthquake. Haiti experienced significant earthquakes in 1751 and 1770 (refs 3–5), but the role of the Enriquillo–Plantain Garden fault zone in these earthquakes is poorly known. We use satellite imagery, aerial photography, light detection and ranging (LIDAR) and field investigations to document Quaternary activity on the Enriquillo–Plantain Garden fault. We report late Quaternary, left-lateral offsets of up to 160 m, and a set of small offsets ranging from 1.3 to 3.3 m that we associate with one of the eighteenth century earthquakes. The size of the small offsets implies that the historical earthquake was larger than M_w 7.0, but probably smaller than M_w 7.6. We found no significant surface rupture associated with the 2010 earthquake. The lack of surface rupture, coupled with other seismologic, geologic and geodetic observations[6,7], suggests that little, if any, accumulated strain was released on the Enriquillo–Plantain Garden fault in the 2010 earthquake. These results confirm that the Enriquillo–Plantain Garden fault remains a significant seismic hazard.

Hispaniola lies along the complex boundary between the North American and Caribbean plates and is therefore subject to large, damaging earthquakes[1–3] (Fig. 1). Caribbean/North American relative plate motion is about 20 mm yr^{-1}, oriented N85° E at the longitude of the Haiti earthquake[8] (Fig. 1). This region is within the transition from a subduction regime to the east to a dominantly strike-slip boundary to the west. Plate motion is partitioned between two offshore thrust systems, the North Hispaniola fault and the Muertos fault, and two major, strike-slip fault zones that bound the intervening Gonave microplate: the Septentrional fault zone (SFZ) on the north and the Enriquillo–Plantain Garden fault zone (EPGFZ) on the south[1,9] (Figs 1 and 2). Geodetically modelled rates for the two strike-slip fault zones are 12 ± 3 mm yr^{-1} for the SFZ, and 6 ± 2 mm yr^{-1} for the EPGFZ (ref. 7). An estimated M_w 8 earthquake on 7 May 1842 probably occurred along the section of the SFZ offshore north of Haiti[3,4]. Palaeoseismic studies on the SFZ indicate a Holocene slip rate of 6–12 mm yr^{-1}, and show that the most recent surface-rupturing earthquake on the central SFZ occurred >800 yr BP, demonstrating a significant seismic hazard[10]. No palaeoseismic studies have been done on the EPGFZ, but historical records suggest that the large (M_w 7.5; refs 3,4) earthquakes of 21 November 1751 and 3 June 1770, which caused severe damage in Port-au-Prince, may have occurred on the EPGFZ, and that a large earthquake on 8 April 1860 may have occurred on this fault farther west along the southern peninsula of Haiti[3,5] (Fig. 1). A large earthquake on 18 October 1751 is associated with the offshore Muertos fault[3,4].

Our study shows that the M_w 7.0 12 January 2010 earthquake generated no significant, through-going, left-lateral surface rupture along the EPGFZ. Instead, the primary geologic signature of this earthquake involved coastal uplift (maximum 0.64 ± 0.11 m) along a 50-km-long section of the coast west of Port-au-Prince[6]. The only surface breaks we found coincident with the EPGFZ occurred near the western end of the aftershock zone where we documented minor, down-to-the-south extensional fractures along a 2.5-km-long section of the fault near Port Royal (Fig. 3; Supplementary Discussion S1). The lack of surface rupture is unusual, given the proximity of the epicentre to the EPGFZ (Fig. 2), the size of the earthquake and the shallow (13 km), oblique strike-slip centroid moment tensor solution[11], but not unprecedented[12]. The 18 October 1989 Loma Prieta, California, earthquake (M_w 6.9) is an example of another similar-size, shallow, oblique-slip earthquake that occurred close to a major strike-slip fault but did not produce surface rupture[13,14]. As the 2010 earthquake in Haiti was not associated with fault surface rupture, it will not leave an easily interpretable signal in the geologic record (Supplementary Discussion S1).

We mapped the Quaternary traces of the EPGFZ on the basis of their geomorphic expression from the western end of the southern peninsula of Haiti near Tiburon to the Dominican Republic border using satellite imagery, light detection and ranging (LIDAR) and aerial photography (Fig. 2a). We also flew aerial reconnaissance along the entire 270-km-length of the fault in Haiti and visited selected field sites between the Dominican Republic border and the Miragoane pull-apart basin. Along most of its length, the fault is topographically well expressed as a strong, linear, N85° E-trending element in the landscape. The fault system includes several prominent stepovers that result in pull-apart basins at extensional left steps and high topographic push-ups at compressional right steps, consistent with active left-lateral strike-slip motion[2] (Fig. 2a).

We focused our field studies on the 110-km-long section of the EPGFZ between Etang Miragoane and the Dominican Republic border (Fig. 2b; Supplementary Discussion S2). The 12 January 2010 epicentre and its aftershocks occurred within this region. For this discussion, we define five fault sections on the basis of differences in geomorphic expression observed during air and ground reconnaissance: from east to west, the Dumay, Momance, Dufort, Goave and Miragoane sections (Fig. 2b; Supplementary Discussion S2). Geomorphic evidence of youthful faulting along the Momance section includes numerous left-laterally offset fluvial

[1]US Geological Survey, 345 Middlefield Road, MS 977, Menlo Park, California 94025, USA, [2]University of Texas Institute for Geophysics, Austin, Texas 78758, USA, [3]US Geological Survey, MS 966, Box 25046, Denver, Colorado 80225, USA, [4]US Geological Survey, 525 S. Wilson Avenue, Pasadena, California 91106, USA, [5]State of Alaska, Geological and Geophysical Surveys, 3354 College Road, Fairbanks, Alaska 99709, USA, [6]Bureau des Mines et de l'Energie, Delmas 19, Rue Nina 14, Box 2174, Port-au-Prince, Haiti. *e-mail: cprentice@usgs.gov.

NATURE GEOSCIENCE DOI:10.1038/NGEO991

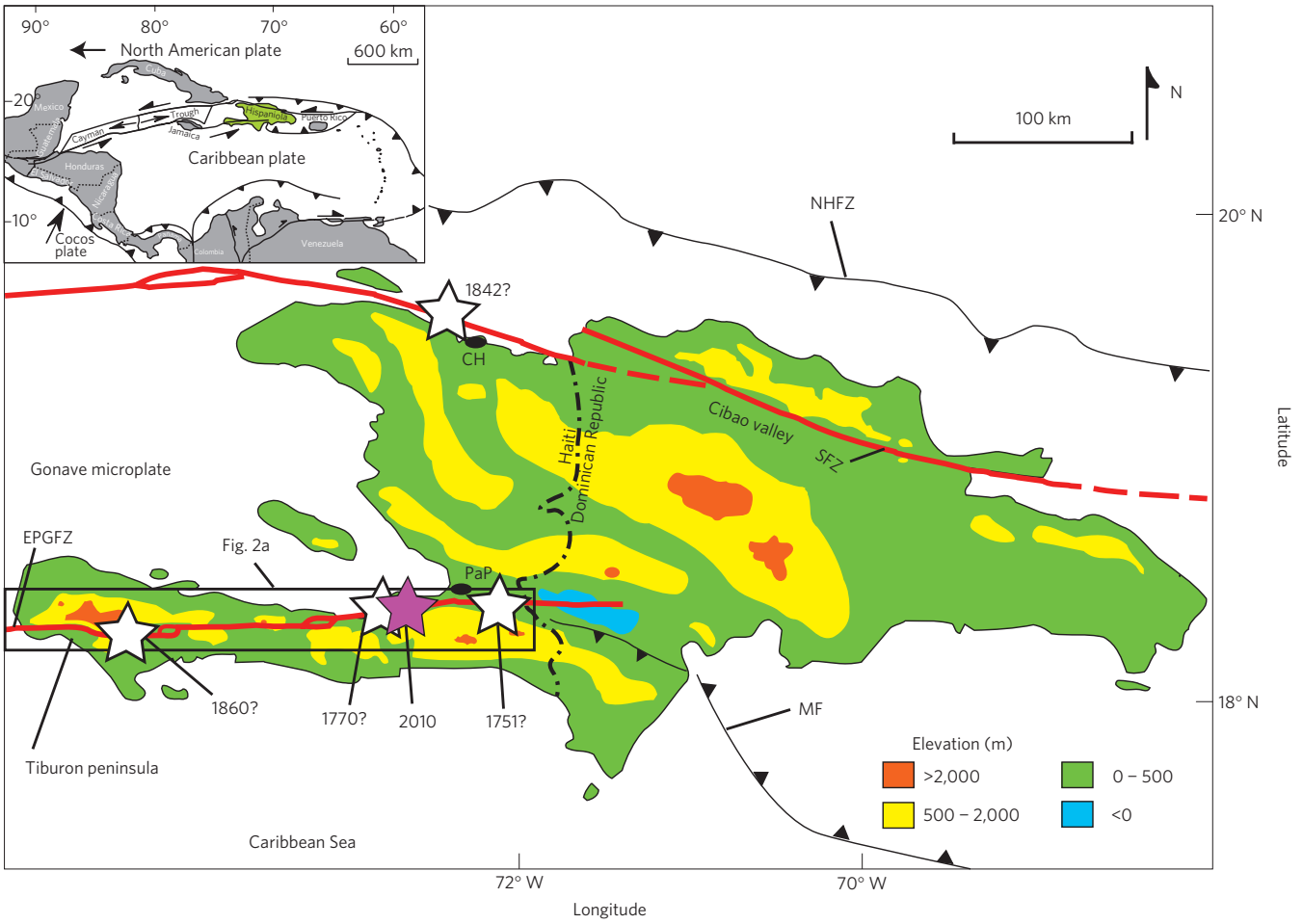

Figure 1 | Tectonic setting of the 12 January 2010 Haiti earthquake. Hispaniola with the two major left-lateral plate-boundary, left-lateral strike-slip faults, the SFZ and the EPGFZ shown in red, which bound the Gonave microplate between the North American and Caribbean plates[1,2]. Thrust fault systems are black lines with teeth on upthrown side. NHFZ = North Hispaniola fault zone. MF = Muertos fault. Purple star = epicentre of the 12 January 2010 earthquake[22]; white stars = estimated epicentres of historical large earthquakes in Haiti[3–5]. PaP = Port-au-Prince; CH = Cap Hatien. The inset shows the main elements of the Caribbean plate boundaries.

channels along a narrow, well-defined, south-dipping fault zone (Supplementary Discussion S3) that coincides with the Rivière Momance valley. We investigated three long-term left-lateral offsets in the field along the Momance and Dumay sections (Supplementary Discussion S4). The geomorphic expression of the fault zone in the Dumay and Dufort sections is more subtle, and consists of diffuse zones of fault-related geomorphic features, suggesting that the most recent surface rupture in these sections may be older than in the Momance section. The Goave section is largely offshore, and is described elsewhere in this issue[15]. The onshore area of the Goave section is marked by a prominent lineament on the south side of Tapion ridge, an area of previous Holocene uplift (Supplementary Discussion S5; Supplementary Table S1). The Miragoane section is characterized by a 5-km-wide left stepover that produces the Mirogoane pull-apart basin.

We identified, mapped and measured nine left-laterally offset streams along a 12-km-long section of the EPGFZ in the valley of Rivière Momance (Fig. 4; Supplementary Table S1). These are the smallest offsets yet observed along the fault (including the Plantain Garden section of the fault studied in Jamaica[16–18]), and we interpret these offsets to result from left-lateral slip during one of the large eighteenth-century earthquakes that occurred on 3 June 1770 and 21 November 1751 (ref. 5). On the basis of historical accounts, researchers have inferred that both earthquakes occurred on the EPGFZ, with estimated M_w 7.5 (refs 3,4). The small offsets are sharp and well preserved, suggesting that they result from a single earthquake, although further palaeoseismic investigations are needed to test this hypothesis. Given the inferred large magnitudes of both events and their close timing, it seems unlikely that both earthquakes ruptured the same section of the fault, leading us to attribute the smallest offsets to only one of these two earthquakes. Our observations provide the first geologic evidence supporting the conclusion that the EPGFZ is the source of at least one of the two eighteenth-century historical events. These small offsets are not visible in any of the high-resolution post-earthquake imagery, emphasizing the importance of field reconnaissance in post-earthquake studies. We constructed a detailed topographic map of the westernmost two small offsets (Figs 4 and 5) where two fault traces offset small channels (Fig. 5a). The southern fault trace offsets channel 1 approximately 2.5 m (Fig. 5b), and the northern trace offsets the channel 1 wall about 0.8 m, indicating a total left-lateral offset of about 3.3 m. We estimate the vertical displacement on the northern trace by projecting the alluvial-fan surface across the scarp, which indicates about 60–75 cm of vertical offset (Fig. 5c). Channel 2 is left-laterally offset about 1.3–2.3 m, with a comparable vertical offset. The remaining seven offsets range from 1.5 to 3.3 m (Fig. 4a; Supplementary Table S1).

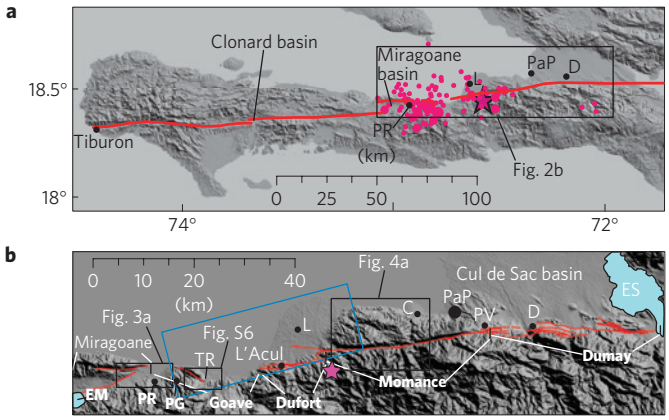

Figure 2 | EPGFZ in southern Haiti. a, Onshore EPGFZ (red lines) from satellite imagery, aerial photography, LIDAR and field observations. The base map is from Shuttle Radar Topography Mission (SRTM) data. D = Dumay, L = Leogane, PaP = Port-au-Prince, PR = Port Royal. Star = epicentre of the 12 January 2010 earthquake[22]. Pink circles = aftershocks $\geq M_w$ 4 from the Advanced National Seismic System[23]; large circles = M_w 6–6.9, intermediate circles = M_w 5–5.9 and small circles = M_w 4–4.9. **b**, Onshore Quaternary traces of the eastern EPGFZ. The fault section boundaries (black vertical bars) are defined by geomorphic changes (Supplementary Discussion S2). Blue rectangle = modelled Leogane fault slip patch at depth[6]. C = Carrefour, D = Dumay, L = Leogane, PaP = Port-au-Prince, PR = Port Royal, PG = Petit Goave, PV = Petionville. The blue areas are lakes: EM = Etang Miragoane, ES = Etang Sumatre. TR = Tapion ridge.

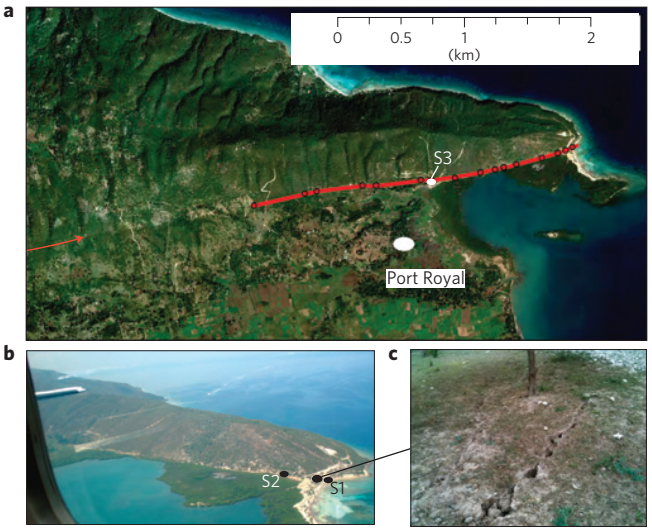

Figure 3 | Surface fractures along the EPGFZ near Port Royal. a, Map showing onshore fractures (red line) along the fault trace. Black circles = global positioning system points along the fracture zone. The base map is a post-earthquake aerial photo acquired by the National Oceanic and Atmospheric Administration. The red arrow marks the continuation of the fault west of the end of the fractures. **b**, Aerial view looking northwestward towards the EPGFZ near Port Royal. The EPGFZ is along the bench near the base of the prominent ridge. **c**, Fractures near coastline. View northeast. Note the right-stepping en echelon extensional fractures, typical of left-lateral slip. This pattern is not consistent, and we found no left-laterally offset features. The dominant mode of slip on 2010 fractures is down-to-the-south extension.

Empirical relations between magnitude and displacement for strike-slip faults worldwide suggest that the average and maximum surface fault displacements for strike-slip earthquakes scale with moment magnitude[19]. The 1.3–3.3 m offsets documented along the Momance section of the EPGFZ are within the expected range for M_w 7.1–7.6 strike-slip earthquakes (Supplementary Discussion S6). We do not have sufficient data to determine whether our measurements either capture the maximum offset or reflect the average offset, but the data do suggest that the average offset is larger than 1.3 m, suggesting an earthquake greater than M_w 7.1. If the largest single-event offset of 3.3 m along the Rivière Momance represents the maximum surface displacement, then the M_w range

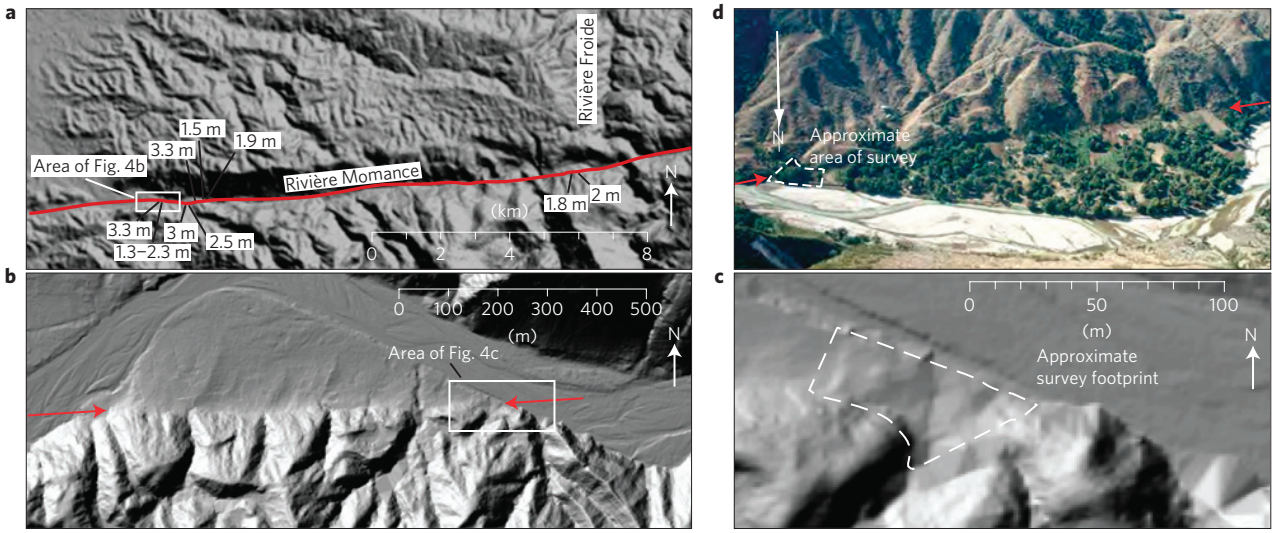

Figure 4 | Locations of small, left-lateral offsets along the Momance section of the EPGFZ. a, Locations of nine small offsets observed in the Momance valley. The base map is from SRTM data. The fault trace is shown by the red line. **b**, Hillshade from LIDAR data showing the area of the topographic survey near Jean-Jean (white rectangle). The fault scarp is between the two red arrows. LIDAR data courtesy of the World Bank, ImageCat and Rochester Institute of Technology Haiti response team; data are freely available at http://ipler.cis.rit.edu/projects/haiti. **c**, Blow-up of the LIDAR image showing the footprint of the survey (white dashes). **d**, Aerial view southward towards the fault scarp (red arrows) near Jean-Jean. The surveyed site is indicated by the white dashes. Small stream offsets are not visible in the aerial photograph because of vegetation.

NATURE GEOSCIENCE DOI:10.1038/NGEO991

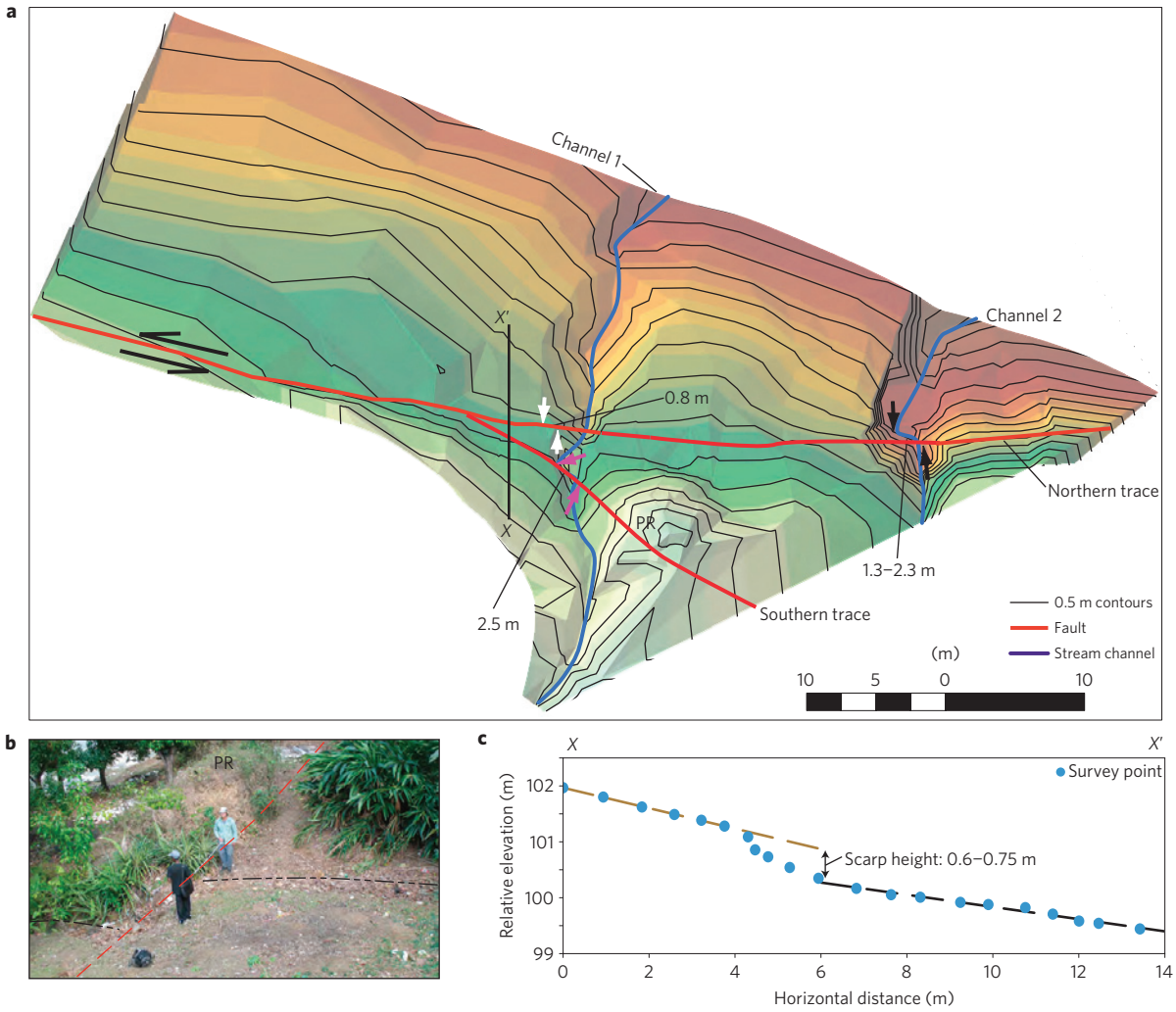

Figure 5 | Detailed topographic survey of small stream offsets at the Jean–Jean site. a, Digital elevation model from total station survey, 0.5 m contours. Green and brown represent higher and lower elevations, respectively. The red lines are fault traces. PR = pressure ridge. The arrows mark offsets: purple and white arrows for channel 1 across the southern and northern traces, respectively; short black arrows for channel 2. **b**, Photograph of channel 1 offset, view eastward. The black dashes mark the thalweg; the red dashes show the southern fault trace. PR = pressure ridge. **c**, Profile *X*–*X*′ across the scarp associated with the northern fault trace. The scarp is eroded back from the fault trace, and is therefore south of the fault.

is 7.1–7.3. We therefore conclude that the earthquake responsible for the smallest documented offsets was larger than M_w 7.0, and probably less than M_w 7.6 (Supplementary Discussion S6). The magnitudes (7.5) and locations (Fig. 1b) assigned to the 3 June 1770 and the 21 November 1751 earthquakes are based on previous analyses of historical damage reports[3–5] and are consistent with our observations of small offsets. We suggest that the small offsets we measured were produced by one of these earthquakes, although at present we cannot confidently determine which of the two events.

The absence of any significant surface rupture associated with the 12 January 2010 earthquake raises the question of which fault is responsible for the event. The epicentral location within a few kilometres of the EPGFZ coupled with the moment tensor showing significant left-lateral slip led to the initial conclusion that the earthquake occurred on the main EPGFZ (ref. 20). However, the absence of significant surface rupture on the EPGFZ opens the possibility that the earthquake occurred on a different structure or structures. Our field observations of the EPGFZ near the epicentre show that the main trace is a south-dipping, left-lateral, strike-slip fault, with a component of up-to-the-south reverse motion (Supplementary Discussion S3). This movement is very different from two proposed fault models for the 12 January 2010 earthquake[6,7]. One of the models uses seismologic, geologic and interferometric synthetic aperture radar (InSAR) data together to suggest slip on three different structures, with 85% of the 12 January 2010 moment release on a north-dipping blind thrust fault, referred to as the Leogane fault[6]. The other fault model also attributes the earthquake to slip on a north-dipping, blind, oblique thrust, on the basis of geodetic data[7]. The Leogane fault may be associated with the Haiti fold-and-thrust belt[21], or could be associated with a complex compressional stepover within the EPGFZ. Our field studies show that near the epicentre in the near surface, the EPGFZ is a high-angle (typically >60°) south-dipping fault that produces left-lateral surface slip during large earthquakes, and therefore is not likely to be the source for the 12 January 2010 earthquake. One of the fault models requires some deep left-lateral slip on a fault near the EPGFZ, so possibly this slip occurred at depth on the EPGFZ, but the model also allows this slip to be on another, subparallel, blind structure[6].

Both fault models suggest that most of the 12 January 2010 moment release was not on the EPGFZ (refs 6,7), which, coupled with our field observations, implies that considerable strain remains

to be released on the EPGFZ. Thus, the EPGFZ remains a serious seismic hazard for Haiti, particularly for the Port-au-Prince area. No slip occurred on the Momance or Dumay sections of the fault east of the epicentre, which are the fault sections closest to Port-au-Prince. Historical records show that no large earthquake has occurred near Port-au-Prince since the earthquakes of 1770 and 1751, and our observations are consistent with surface rupture on the Momance section of the EPGFZ associated with one of these events. The 12 January 2010 earthquake did not release any strain accumulated since the last earthquake on the Momance or Dumay sections, and may not have fully released accumulated shear strain on the Dufort, Goave or Miragoane sections either. These sections of the fault remain capable of generating an earthquake $>M_w$ 7.0, and, in the case of the Momance and Dumay sections, which are closer to Port-au-Prince, potentially causing stronger ground shaking in the urban area than the 12 January event.

Received 23 May 2010; accepted 27 September 2010; published online 24 October 2010

References

1. Mann, P., Matumoto, T. & Burke, K. Neotectonics of Hispaniola—Plate motion, sedimentation, and seismicity at a restraining bend. *Earth Planet. Sci. Lett.* **70,** 311–324 (1984).
2. Mann, P., Taylor, F. W., Edwards, R. L. & Ku, R. Actively evolving microplate formation by oblique collision and sideways motion along strike-slip faults: An example from the northeastern Caribbean plate margin. *Tectonophysics* **246,** 1–69 (1995).
3. McCann, W. R. in *Caribbean Tsunami Hazard* (eds Aurelio, M. & Philip, L.) 43–65 (World Scientific, 2006).
4. Ali, S. T., Freed, A. M., Calais, E., Manaker, D. M. & McCann, W. R. Coulomb stress evolution in northeastern Caribbean over the past 250 years due to coseismic, postseismic, and interseismic deformation. *Geophys. J. Int.* **174,** 904–918 (2008).
5. Scherer, J. Great earthquakes in the island of Haiti. *Bull. Seismol. Soc. Am.* **2,** 174–179 (1912).
6. Hayes, G. P. *et al.* Complex rupture during the 12 January 2010 Haiti earthquake. *Nature Geosci.* **3,** 800–805 (2010).
7. Calais, E. *et al.* The January 12, 2010, M_w 7.0 earthquake in Haiti: Context and mechanism from an integrated geodetic study. *Nature Geosci.* **3,** 794–799 (2010).
8. Manaker, D. M. *et al.* Interseismic plate coupling and strain partitioning in the Northeastern Caribbean. *Geophys. J. Int.* **174,** 889–903 (2008).
9. Dolan, J. F. & Wald, D. J. in *Active Strike-Slip and Collisional Tectonics of the Northern Caribbean Plate Boundary Zone* (eds Dolan, J. F. & Mann, P.) 143–169 (Geol. Soc. Am. Special Paper, Vol. 326, 1998).
10. Prentice, C. S., Mann, P., Peña, L. & Burr, G. Slip rate and earthquake recurrence along the central Septentrional fault, North American–Caribbean plate boundary, Dominican Republic. *J. Geophys. Res.* **108,** 2149–2165 (2003).
11. USGS cenroid moment solution: http://earthquake.usgs.gov/earthquakes/eqinthenews/2010/us2010rja6/neic_rja6_cmt.php.
12. Wesnousky, S. G. Displacement and geometrical characteristics of earthquake surface ruptures; issues and implications for seismic-hazard analysis and the process of earthquake rupture. *Bull. Seismol. Soc. Am.* **98,** 1609–1632 (2008).
13. Arnadottir, T. & Segall, P. The 1989 Loma Prieta earthquake imaged from the inversion of geodetic data. *J. Geophys. Res.* **99,** 21835–21855 (1994).
14. Prentice, C. S. & Schwartz, D. P. Re-evaluation of 1906 surface faulting, geomorphic expression, and seismic hazard along the San Andreas fault in the southern Santa Cruz Mountains. *Bull. Seismol. Soc. Am.* **81,** 1424–1479 (1991).
15. Hornbach, M. J. *et al.* Uplift, sliding, and tsunamigenesis along a strike-slip fault. *Nature Geosci.* **3,** 783–788 (2010).
16. Mann, P. *et al. 18th Caribbean Geological Conf. 24–28 March, 2008, Santo Domingo, Dominican Republic* http://www.ig.utexas.edu/jsg/18_cgg/Mann3.htm (2008).
17. Mann, P. *et al.* Late Quaternary activity and seismogenic potential of the Gonave microplate: Plantain Garden strike-slip fault zone of eastern Jamaica. *Eos Trans. AGU (Fall Meeting Suppl.)* **89,** abstr. T11B-1869 (2008).
18. Koehler, R. D., Mann, P. & Brown, L. A. Tectonic geomorphology and paleoseismology of strike-slip faults in Jamaica: Implications for distribution of strain and seismic hazard along the southern edge of the Gonave microplate. *Eos Trans. AGU (Fall Meeting Suppl.)* **90,** abstr. G33B-0658 (2009).
19. Wells, D. L. & Coppersmith, K. J. New empirical relationships among magnitude, rupture length, rupture width, rupture area, and surface displacement. *Bull. Seismol. Soc. Am.* **84,** 974–1002 (1994).
20. For example, see initial USGS online summary report: http://earthquake.usgs.gov/earthquakes/recenteqsww/Quakes/us2010rja6.php#summary.
21. Pubellier, M., Mauffret, A., Leroy, S., Vlia, J. M. & Amilcar, H. Plate boundary readjustment in oblique convergence: Example of the Neogene of Hispaniola, Greater Antilles. *Tectonics* **19,** 630–648 (2000).
22. Earthquake epicenter from USGS: http://earthquake.usgs.gov/earthquakes/recenteqsww/Quakes/us2010rja6.php.
23. Advanced National Seismic System (ANSS) website, catalog search: www.ncedc.org/anss/catalog-search.html.

Acknowledgements

We thank the Haitian Bureau of Mines and Energy, especially D. Anglade, for invaluable assistance. We are indebted to R. Boyer, R. Arbouet, Jr. and A. Chery for field assistance. We also thank L. Blair, R. Renaldo and N. Knepprath (USGS) for GIS support. The US Agency for International Development (USAID) Office of Foreign Disaster Assistance and the US Geological Survey (USGS) National Earthquake Hazards Reduction Program provided funds for the USGS-USAID Earthquake Disaster Assistance Team (EDAT) to carry out this work. Financial support was also provided by the National Science Foundation (grant EAR1024990 to P.M.). UTIG contribution 2284. We thank S. Hough and M. Tuttle for helpful and constructive criticism of earlier versions of this manuscript.

Author contributions

C.S.P. was responsible for writing the manuscript and generating most of the figures, with input from all authors. R.D.G. reduced the survey data collected by C.S.P. and A.J.C. to produce the map that appears in Fig. 5, and contributed substantially to Fig. 4b,c. C.S.P., R.D.G. and A.J.C. contributed to interpretation of survey data. C.S.P., R.D.G. and K.W.H. contributed text and figures to the Supplementary Information, which was coordinated by C.S.P. All authors collected data in the field and contributed to data analysis and synthesis.

Additional information

The authors declare no competing financial interests. Supplementary information accompanies this paper on www.nature.com/naturegeoscience. Reprints and permissions information is available online at http://npg.nature.com/reprintsandpermissions. Correspondence and requests for materials should be addressed to C.S.P.